



Effects of lithium salts on PEO-based solid polymer electrolytes and their all-solid-state lithium-ion batteries

Yi Zhang¹ · Wei Feng¹ · Yichao Zhen¹ · Peiyao Zhao¹ · Xiaohui Wang¹ · Longtu Li¹

Received: 3 February 2022 / Revised: 10 March 2022 / Accepted: 14 March 2022 / Published online: 30 March 2022
© The Author(s), under exclusive licence to Springer-Verlag GmbH Germany, part of Springer Nature 2022

Abstract

For all-solid-state lithium-ion batteries (ASSBs), they have two key parameters including ionic conductivity and interfacial properties. Considering the previous studies focused more on single property, we aimed to investigate the effects of lithium salts on comprehensive properties of PEO-based SPEs and find out the optimal lithium salts. For the SPE with LiTFSI, it has the highest ionic conductivity ($5.3 \times 10^{-6} \text{ S cm}^{-1}$ at 25 °C and $2.4 \times 10^{-4} \text{ S cm}^{-1}$ at 60 °C) and discharge capacity, mainly due to the lowest crystallinity and the highest lithium-ion transference number. For the SPE with LiFSI, it has the best interfacial properties and cycling performance, mainly due to the denser and flatter LiF SEI layer after cycling. Our work indicates that as for PEO-based ASSBs, LiTFSI can be used to get higher discharge capacities, and LiFSI can be used to get higher retention rate.

Keywords PEO-based solid polymer electrolytes · All-solid-state lithium-ion batteries · Ionic conductivity · Interfacial properties · Lithium salts

Introduction

All-solid-state lithium-ion batteries (ASSBs) have been considered in order to improve the energy density and the safety of lithium-ion batteries. ASSBs use solid electrolytes (SEs) instead of liquid electrolytes, but the resulting problems of rate performance and cycling stability need to be solved [1–3]. Among these problems, SE-electrode interfacial property is addressed as one of the key issues [4].

SEs can be classified into three groups, including polymer-based, sulfide-based, and oxide-based [5]. For solid polymer electrolytes (SPEs), previous studies focus more on how to increase the ionic conductivity, such as adding nanoparticles and modifying polymer chains [6–8]. However, the comprehensive performance of SPEs and their ASSBs depends on not only ionic conductivity, but also interfacial properties [9]. Therefore, in order to make ASSBs commercialized successfully, interfacial properties should be further improved.

Interfacial phenomena of SE-electrode interface can be classified into two aspects [10]. One aspect is due to physical factors, mainly caused by rigid contact. In this aspect, SE-electrode interface is not fully contact, even when there is point-contact interface, especially for oxide-based electrolytes [11, 12]. The other aspect is due to chemical factors, mainly caused by the reaction in the interface and the decomposition of SEs [13–15]. In terms of other previous studies, physical factors of PEO-based SPEs can be solved by hot pressed or interface engineering, so they can fit on electrodes tightly [16–18]. As a result, chemical factors can dominate interfacial properties, and lithium salts have significant effects on chemical factors, especially for the SPEs-anode interface [19, 20].

✉ Xiaohui Wang
wxh@tsinghua.edu.cn

Yi Zhang
zyi17@mails.tsinghua.edu.cn

Wei Feng
13080684589@163.com

Yichao Zhen
yczhen186@163.com

Peiyao Zhao
15652790625@163.com

Longtu Li
llt-dms@mail.tsinghua.edu.cn

¹ State Key Laboratory of New Ceramics and Fine Processing, School of Materials Science and Engineering, Tsinghua University, Beijing 100084, People's Republic of China

For PEO-based ASSBs, their compatible lithium salts are different with liquid lithium-ion battery (LIB). This is due to that inorganic lithium salts, such as LiPF_6 and LiBF_4 , have bad thermal stability; some irreversible reactions take place easily above $50\text{ }^\circ\text{C}$, resulting in decomposition during cycling [21]. For organic lithium salts, their decomposition temperature is above $200\text{ }^\circ\text{C}$, indicating they have good thermal stability [22–24]. As a result, it is necessary to find out optimal lithium salts and their effects on PEO-based SPEs. Previous studies have investigated the interfacial properties of liquid lithium-ion battery and found out that LiFSI is the best lithium salt, because its decomposition product is LiF, which can induce the construction of stable solid electrolyte interface (SEI) [25]. However, there is less research on whether LiF has such an effect on ASSBs and the formation of SEI for different lithium salts in ASSBs. Besides, previous works focus more on single properties of SPEs; there is less research about the effects of lithium salts on comprehensive properties of PEO-based SPEs. Consequently, effects of lithium salts on PEO-based electrolytes were systematically explored in this work. For organic lithium salts, LiTFSI, LiFSI, and $\text{CF}_3\text{SO}_3\text{Li}$ have high ionic conductivity and ease of preparation, so three lithium salts are widely used in PEO-based SPE, and we chose these three in our work [22–24].

Experimental procedures

Preparation of membranes

For PEO-based SPEs with different lithium salts, they were prepared by solution casting. First, polyethylene oxide (PEO, $1 \times 10^6\text{ g mol}^{-1}$, Aladdin), bis (trifluoromethanesulfonyl) imide lithium (LiTFSI, Aladdin), bis (fluorsulfonyl) imide lithium (LiFSI, Aladdin), and lithium trifluoromethanesulfonate ($\text{CF}_3\text{SO}_3\text{Li}$, Aladdin) were dried for 24 h at $60\text{ }^\circ\text{C}$. Then, PEO and different lithium salts with a fixed molar ratio of 16:1 were added into acetonitrile (ACN, Aladdin), which was packed in a closed container to avoid the mixture contact with air and water. After stirring for 24 h, the mixture was cast into a Teflon plate and dried for 48 h. Finally, SPEs were peeled off and then hot pressed at $60\text{ }^\circ\text{C}$ to make them smooth and flat.

Characterization

X-ray diffraction (XRD, Rigaku 2500, Kyoto, Japan) was performed with $\text{Cu K}\alpha$ radiation ($\lambda = 1.5418\text{ \AA}$) over the 2θ

range of $10^\circ\text{--}70^\circ$. In order to determine the crystallinity (χ_c) of SPEs, differential scanning calorimeter (DSC, Netzsch, Selb, Germany) measurement was performed in the temperature range of 20 to $80\text{ }^\circ\text{C}$, and values of crystallinity were calculated as the Eq. 1:

$$\chi_c = \frac{\Delta H_m / \phi}{\Delta H_m^*} \times 100\% \quad (1)$$

In this equation, ΔH_m is the melting enthalpy of each SPE, ΔH_m^* is the melting enthalpy of fully crystallized PEO with the value of 177.8 J g^{-1} , and ϕ is the mass fraction of PEO matrix [26].

Ionic conductivity (σ) is one of the most important parameters of SPEs, and it was measured by an electrochemical work station (CHI660D, Shanghai Chenhua instrument Co., Ltd., China) in the frequency range of 0.1 Hz to 1 MHz . The measurement was performed with the stainless-steel (ss)//SPE//ss, and values of ionic conductivity were calculated as following:

$$\sigma = \frac{L}{R_b S} \quad (2)$$

As shown in Eq. 2, L , R_b , and S are thickness, bulk resistance, and area of SPEs respectively [27].

The activation energy (E_a) of SPEs was evaluated to find out the relationship between ionic conductivity and temperature, and values were calculated by the Eq. 3:

$$\sigma = A \exp\left(\frac{-E_a}{KT}\right) \quad (3)$$

where A , K , and T are pre-exponential constant, Boltzmann constant, and absolute temperature respectively [28].

In order to determine the electrochemical stability window, linear sweep voltammetry (LSV) measurement was performed in the voltage range of 0 to 6 V at $60\text{ }^\circ\text{C}$.

In order to determine the interfacial properties, galvanostatic cycling was measured in different currents at $60\text{ }^\circ\text{C}$. In this measurement, Li//SPEs with different salts//Li symmetry cells were assembled, and charge/discharge cycling was periodically changed per 0.5 h . Later, X-ray photoelectron spectroscopy (XPS, ESCALAB 250Xi, Thermo Fisher, America) measurement was performed to find out the changes in the interface.

Cycling performance of ASSBs was measured on a battery testing instrument (CT3001K, LANHE, Wuhan) at $60\text{ }^\circ\text{C}$. First, LiFePO_4 (LFP) cathode material was made up of $70\text{ wt}\%$ LFP powder (with the tap density of 1.1 g cm^{-3} , Aladdin), $20\text{ wt}\%$ Super-P (Aladdin), and $10\text{ wt}\%$ Polyvinylidene fluoride (PVDF, $1 \times 10^6\text{ g mol}^{-1}$, Aladdin), which the cathode loading was 2 mg cm^{-2} . Then, LFP//SPEs//Li cells were assembled. Finally, charge/discharge cycling was tested to find out the effects of lithium salts on SPEs.

Fig. 1 **a** XRD patterns and **b** DSC curves of SPEs with different lithium salts

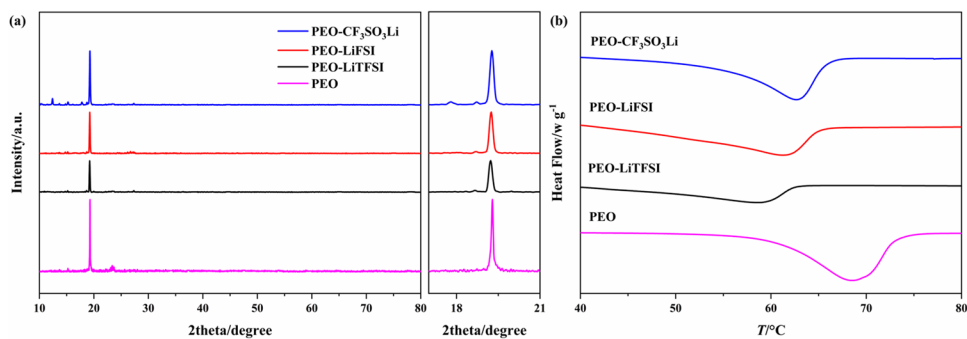


Table 1 Values of ΔH_m and χ_c of different SPEs

SPEs	$\Delta H_m / \text{J g}^{-1}$	$\chi_c / \%$
PEO	-147.40	82.90
PEO-LiTFSI	-50.28	28.29
PEO-LiFSI	-60.31	33.93
PEO-CF ₃ SO ₃ Li	-80.21	45.12

Results and discussion

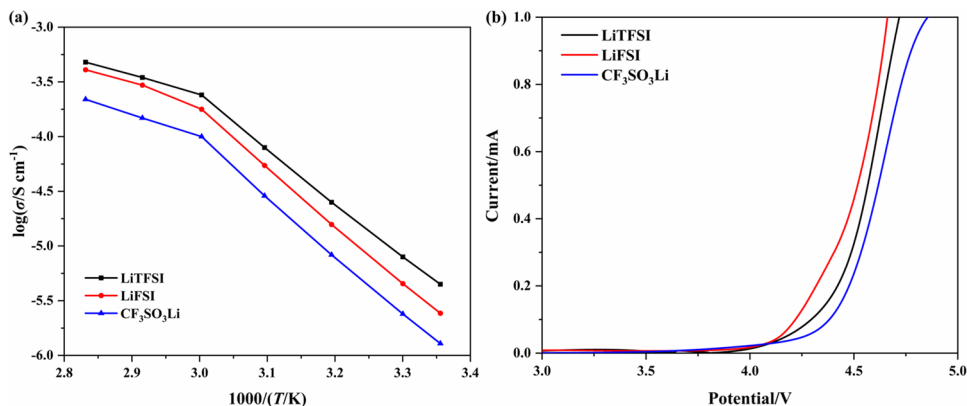
Phase structure and crystallinity analysis

Figure 1a shows the XRD patterns of SPEs with different salts. From the patterns, each SPE has the same characteristic peak position ($2\theta = 19.2^\circ$). Meanwhile, diffraction peak intensity of each PEO matrix is mutually different, indicating crystallinity of each SPE is different. DSC curves are shown in Fig. 1b, and values of crystallinity are shown in Table 1. Consistent with the results from XRD patterns, crystallinity of PEO-LiTFSI is the lowest, so it has the weakest characteristic diffraction peak in Fig. 1a.

Electrochemical measurement of SPEs

As mentioned above, ionic conductivity is one of the key parameters of SPEs. Figure 2a shows the ionic conductivity of SPEs with different lithium salts; all the values are

Fig. 2 **a** Ionic conductivity and **b** linear sweep voltammetry of SPEs at 60 °C



shown in Table 2. From Fig. 2a, SPEs with LiTFSI have the highest ionic conductivity, mainly caused by the following reasons: On the one hand, according to the results from XRD and DSC measurement, SPEs with LiTFSI have the lowest crystallinity, due to the plasticizing effect caused by the high flexibility of TFSI⁻ [29]. Previous studies demonstrate that pathways of lithium-ions conduction are mainly in amorphous regions of PEO-based SPEs [30]. As a result, the lower the crystallinity is, the higher the ionic conductivity will be. On the other hand, according to the results from Table S1 and Fig. S1, SPEs with LiTFSI have the highest lithium-ion transference number (t_{Li^+}), further improving the ionic conductivity.

Figure 2b shows the linear sweep voltammetry of SPEs with different salts. As shown in Fig. 2b, the electrochemical window of SPEs with different salts is below 4.0 V; as a result, they cannot match LiCoO₂ (LCO) and NCM cathodes.

Interfacial properties analysis

The interfacial property is another key parameter of SPEs. In order to find out the effects of lithium salts on interfacial properties, the relationship between interfacial resistance of each SPE and storage days was measured, and results are shown in Fig. 3. It can be seen that interfacial resistance of each SPE decreases during the first day, which is due to the contact improvement between SPEs and Li metal.

Table 2 Values of the σ and E_a of different SPEs at 60 °C

SPEs	$\sigma(25\text{ °C})/S\text{ cm}^{-1}$	$\sigma(60\text{ °C})/S\text{ cm}^{-1}$	$E_a(\text{below } 50\text{ °C})/KJ\text{ mol}^{-1}$	$E_a(\text{above } 50\text{ °C})/KJ\text{ mol}^{-1}$
PEO-LiTFSI	5.3×10^{-6}	2.4×10^{-4}	93.9	33.5
PEO-LiFSI	2.4×10^{-6}	1.8×10^{-4}	101.1	38.0
PEO-CF ₃ SO ₃ Li	1.3×10^{-6}	1.0×10^{-4}	102.6	40.2

Later, interfacial resistance of each SPE increases continually, which is due to the decomposition of lithium salts, and the related mechanism is analyzed in the following. Besides, PEO-LiFSI has the lowest interfacial resistance in each storage day, indicating PEO-LiFSI has the best interfacial property. Furthermore, galvanostatic cycling was measured at different currents (0.1 mA cm^{-2} , 0.2 mA cm^{-2} , and 0.5 mA cm^{-2}) at 60 °C. In this measurement, symmetry cells

were assembled with the structure of Li//SPEs with different lithium salts//Li. Figure 3b shows the voltage profiles at a current density of 0.1 mA cm^{-2} : On the one hand, polarization voltages of all SPEs remain stable in 1000 cycles, which means cycles of all ASSBs lasted for 1000 times. On the other hand, polarization voltages of SPEs with LiFSI are always the lowest, indicating the lowest interface resistance. Figure 3c shows the voltage profiles at 0.2 mA cm^{-2} ,

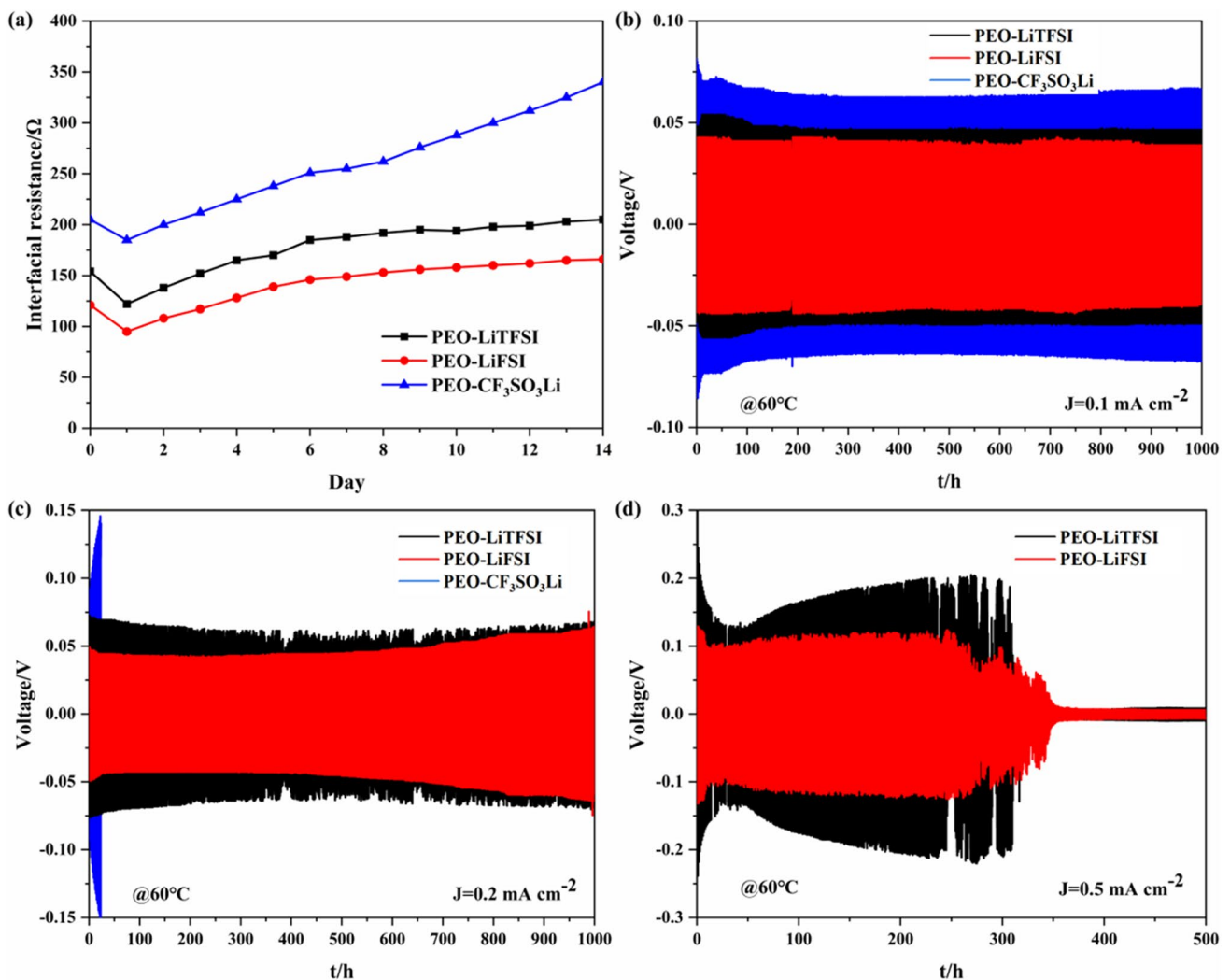
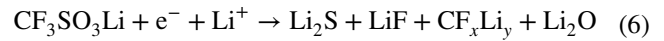
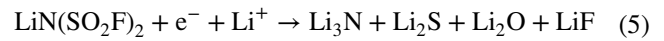
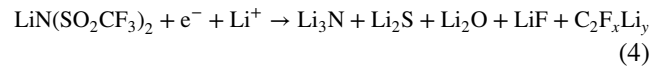


Fig. 3 a The relationship between interfacial resistance and storage days; voltage profiles of galvanostatic cycling for Li//SPEs with different salts//Li symmetry cells at the current density of **b** 0.1 mA cm^{-2} , **c** 0.2 mA cm^{-2} , and **d** 0.5 mA cm^{-2} at 60 °C

cycles of SPEs with LiTFSI and LiFSI lasted for 1000 times, and the former is fluctuant during cycling, and the latter is always stable. However, the polarization voltage of SPEs with CF₃SO₃Li increases rapidly in the first 30 cycles, indicating they cannot be used under larger current density. Figure 3d shows the voltage profiles at 0.5 mA cm⁻², and both SPEs have similar phenomena: cycles of SPEs with LiTFSI and LiFSI lasted for 300 times with fluctuation and decreased rapidly after 300 cycles, indicating both ASSBs were short-circuited caused by lithium dendrites.

Furthermore, in order to determine the mechanism of these phenomena, XPS measurements were performed on pristine SPEs and cycled SPEs to explore the change of SPEs-Li interface after galvanostatic cycling. Figure 4a–d show the XPS spectra of C 1 s, O 1 s, F 1 s, and S 2p of pristine SPEs and cycled SPEs. In Fig. 4c, F atom exists as LiF and LiFSI, and peaks of FSI⁻ nearly disappear after Ar sputter, indicating FSI⁻ has broken down in the interface. Meanwhile, peaks of Li₂CO₃, LiF, and Li₂S are more significant after Ar sputter, indicating the decomposition materials of LiFSI are LiF, Li₂CO₃, and Li₂S. As shown in Fig. S2 to S3, LiTFSI and CF₃SO₃Li also break down into different lithium salts in the interface. Previous studies identified the formation of the SEI layer is related to

the decomposition of PEO and determined by the decomposition of lithium salts [31, 32]. Corresponding to the mechanism of lithium salt decomposition in the interface, chemical equations are shown as Eqs. 4, 5, and 6 respectively, resulting in the difference of interfacial resistance [33–35]:



In order to find out the reason for interfacial property differences of SPEs with different salts, atomic abundance of the cycled SPEs have measured. For SPEs with different lithium salts, the abundance of F and LiF can be determined from XPS spectra, and values are shown in Table 3. From Table 3, no matter how long the sputter time is, the order of LiF abundance is LiFSI > LiTFSI > CF₃SO₃Li in the interface. Based on previous research, LiF has the largest bandgap (13.6 eV), so LiF SEI layer can stop electron tunneling and increase the interfacial properties [36, 37].

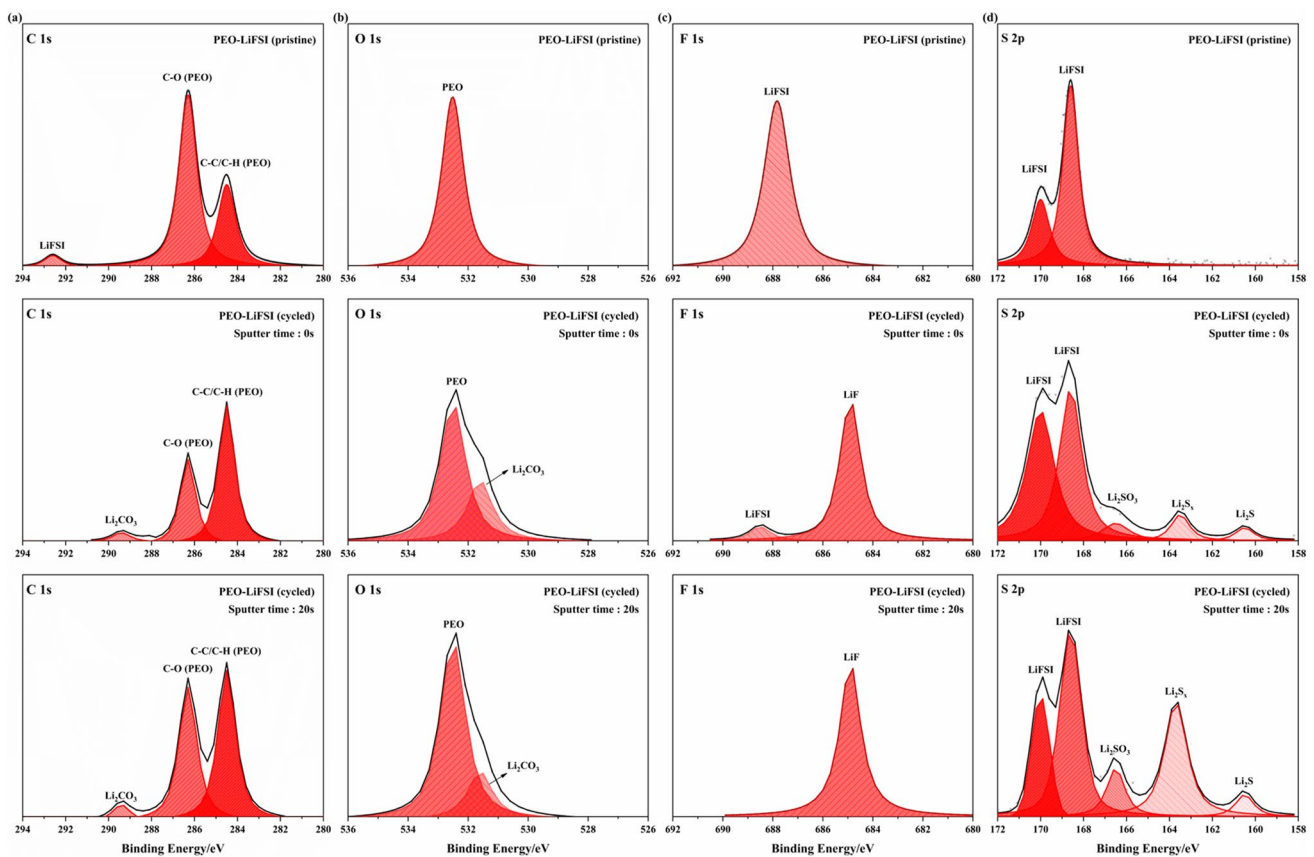


Fig. 4 XPS spectra of **a** C 1 s, **b** O 1 s, **c** F 1 s, and **d** S 2p of pristine SPEs and cycled SPEs with LiFSI after Ar sputter for different times

Table 3 LiF abundance of cycled SPEs with different lithium salts

SPEs	Sputter time	Molar ratio of F atom	Molar ratio of LiF
SPEs with LiTFSI	0 s	5.17%	0.71%
SPEs with LiTFSI	120 s	12.84%	8.66%
SPEs with LiFSI	0 s	4.87%	4.41%
SPEs with LiFSI	120 s	10.91%	10.91%
SPEs with CF ₃ SO ₃ Li	0 s	5.14%	3.78%
SPEs with CF ₃ SO ₃ Li	120 s	7.60%	5.91%

Therefore, the more the content of LiF is, the better the interfacial properties will be. Besides, LiF SEI layer is dense and flat, resulting in the closer contact between Li foils and SPEs [25]. Post-mortem analysis was made to investigate the mechanism of interfacial performance differences of PEO-based SPEs with different lithium salts, and SEM micrographs of cycled SPEs are shown in Fig. 5.

Surface morphology of the cycled SPE with LiFSI and its matching Li foil is denser and flatter than others, indicating the SEI layer of LiFSI is denser and flatter than others, caused by the uniform deposition of LiF. As a result, SPEs with LiFSI have the best interfacial properties.

Cell performance of SPEs

In order to investigate the cell performance, LiFePO₄/SPEs with different lithium salts/Li ASSBs were assembled. Figure 6a shows the cycling performance of ASSBs at 0.1 C rate. In Fig. 6a, the cell with LiTFSI always has the highest discharge capacities, due to the highest ionic conductivity. For the cell with LiFSI, although its discharge capacities are lower than the former, it has the highest retention rate (84.3%, corresponding to 78.8% for the former), caused by the best interfacial properties.

Figure 6b and c show charge/discharge curves after first and 100 cycles respectively. For initial charge/discharge cycle, polarization voltages of all SPEs are nearly same,

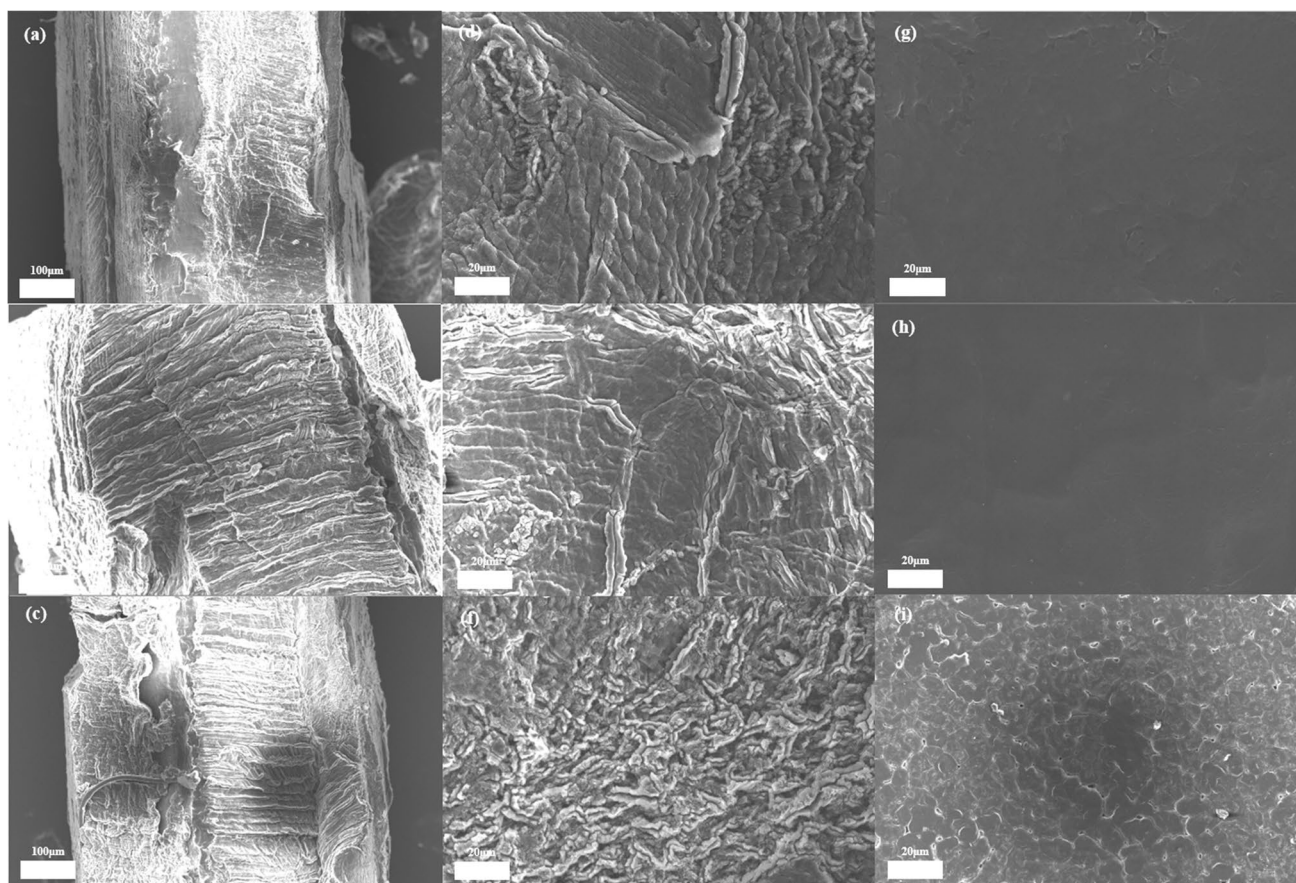


Fig. 5 SEM micrographs of cross-section of Li//SPEs//Li symmetric cells at the current density of 0.1 mA cm⁻² after 100 cycles with **a** LiTFSI, **b** LiFSI, and **c** CF₃SO₃Li. SEM micrographs of Li foils of Li//SPEs//Li symmetric cells at the current density of 0.1 mA cm⁻²

after 100 cycles with **d** LiTFSI, **e** LiFSI, and **f** CF₃SO₃Li. SEM micrographs of SPEs of Li//SPEs//Li symmetric cells at the current density of 0.1 mA cm⁻² after 100 cycles with **g** LiTFSI, **h** LiFSI, and **i** CF₃SO₃Li

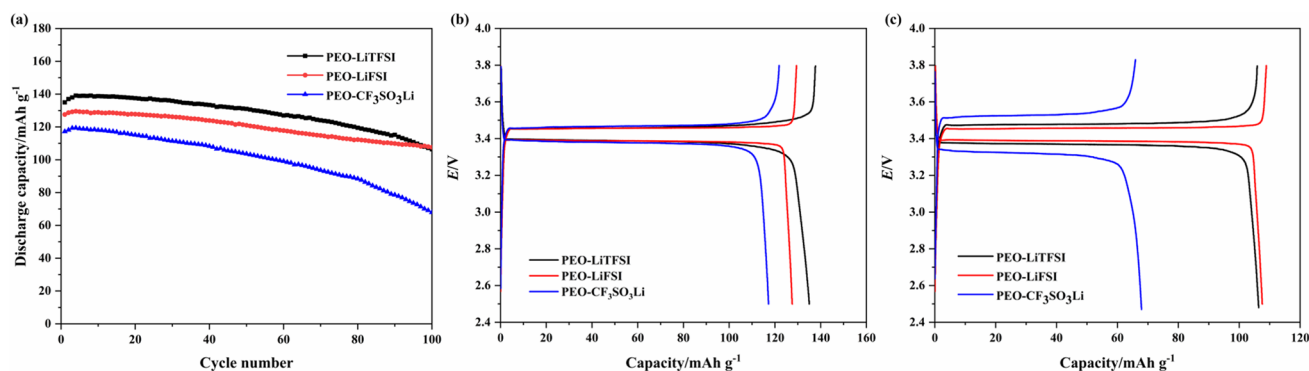


Fig. 6 **a** Cycling performance of ASSBs with different SPEs, **b** initial charge/discharge curves, and **c** charge/discharge curves after 100 cycles of different ASSBs

indicating the same interface resistance after the first cycle. After 100 cycles, polarization voltage of the cell with LiFSI is the lowest, consisting with the highest retention rate in Fig. 6a. These phenomena reveal that retention rate and cycling stability mainly depend on interfacial properties, which is determined by lithium salts. Also, LiTFSI can be used to get higher discharge capacities, and LiFSI can be used to get higher retention rate.

Conclusion

In this work, we aimed to find out the effects of lithium salt on PEO-based SPEs and their ASSBs. PEO-based SPEs with different lithium salts were synthesized by solution casting; Li//SPEs//Li symmetry cells and LFP//SPEs//Li ASSBs were assembled to investigate the cycling performance. Based on our study, for the SPE with LiTFSI, it has the highest ionic conductivity ($5.3 \times 10^{-6} \text{ S cm}^{-1}$ at 25°C and $2.4 \times 10^{-4} \text{ S cm}^{-1}$ at 60°C) and discharge capacity, mainly due to the lowest crystallinity and the highest lithium-ion transference number. For the SPE with LiFSI, it has the best interfacial properties and cycling performance, mainly due to the denser and flatter LiF SEI layer after cycling. Our work indicates that as for PEO-based ASSBs, LiTFSI can be used to get higher discharge capacities, and LiFSI can be used to get higher retention rate.

Supplementary Information The online version contains supplementary material available at <https://doi.org/10.1007/s11581-022-04525-3>.

Funding This work was supported by National Natural Science Foundation of China (Grant No. 52032005), Ministry of Sciences and Technology of China through National Basic Research Program of China (973 Program 2015CB654604).

References

- Scrosati B, Garche J (2010) Lithium batteries: status, prospects and future. *J Power Sources* 195:2419–2430
- Trapa PE, Won YY, Mui SC, Olivetti EA, Huang BY, Sadoway DR, Mayes AM, Dallek S (2005) Rubbery graft copolymer electrolytes for solid-state, thin-film lithium batteries. *J Electrochem Soc* 152:1–5
- Croce F, Appetecchi GB, Persi L, Scrosati B (1998) Nanocomposite polymer electrolytes for lithium batteries. *Nature* 394:456–458
- Zhu B, Jin Y, Hu XZ, Zheng QH, Zhang S, Wang QJ, Zhu J (2016) Poly(dimethyl siloxane) thin film as a stable interfacial layer for high-performance lithium-metal battery anodes. *Adv Mat* 29:1603755
- Fergus JW (2010) Ceramic and polymeric solid electrolytes for lithium-ion batteries. *J Power Source* 195:4554–4569
- Zheng J, Tang MX, Hu YY (2016) Lithium-ion pathway within $\text{Li}_7\text{La}_3\text{Zr}_2\text{O}_{12}$ -polyethylene oxide. *Angew Chem* 55:1–6
- Aldalur I, Martinez M, Krzton A, Piszcz M, Armand M, Zhang H (2019) Flowable polymer electrolytes for lithium metal batteries. *J Power Source* 423:218–226
- Wang QJ, Song WL, Fan LZ, Shi Q (2015) Effect of alumina on triethylene glycol diacetate-2-propenoic acid butyl ester composite polymer electrolytes for flexible lithium ion batteries. *J Power Sources* 279:405–412
- Ismail I, Noda A, Nishimoto A, Watanabe M (2001) XPS study of lithium surface after contact with lithium-salt doped polymer electrolytes. *Electrochim Acta* 46:1595–1603
- Yamada H (2016) Interfaces of solid electrolytes: fundamentals and applications. *J Indian Inst Sci* 96:315–323
- Ohta S, Komagata S, Seki J, Saeki T, Morishita S, Takahiro A (2013) All-solid-state lithium ion battery using garnet-type oxide and Li_3BO_3 solid electrolytes fabricated by screen-printing. *J Power Source* 238:53–56
- Liu LL, Xu JR, Wang S, Wu F, Li H, Chen LQ (2019) Practical evaluation of energy densities for sulfide solid-state batteries. *eTransportation* 1:100010
- Liu Z, Qi Y, Lin YX, Chen L, Lu P, Chen LQ (2016) Interfacial study on solid electrolyte interphase at Li metal anode: Implication for Li dendrite growth. *J Electrochem Soc* 163:592–598
- Naoi K, Mori M, Naruoka Y, Lamanna W, Atanasoski R (1999) The surface film formed on a lithium metal electrode in a new imide electrolyte, lithium bis(perfluoroethylsulfonylimide) [$\text{Li}(\text{C}_2\text{F}_5\text{SO}_2)_2$]. *J Electrochem Soc* 146:462–469

15. Wu BB, Wang SY, Lochala J, Desrochers D, Liu B, Zhang WQ, Yang JH, Xiao J (2018) The role of the solid electrolyte interphase layer in preventing Li dendrite growth in solid-state batteries. *Energy Environ Sci* 11:1803–1810
16. Yang G, Zhai Y, Yao J, Song S, Lin L, Tang W, Wen Z, Hu N, Lu L (2021) Synthesis and properties of poly(1,3-dioxolane) in situ quasi-solid-state electrolytes via a rareearth triflate catalyst. *Chem Commun* 57:7934–7937
17. Zhai Y, Yang G, Zeng Z, Song S, Li S, Hu N, Tang W, Wen Z, Lu L, Molenda J (2021) Composite hybrid quasi-solid electrolyte for high-energy lithium metal batteries. *ACS Appl Energy Mater* 4:7973–7982
18. Song S, Gao W, Yang G, Zhai Y, Yao J, Lin L, Tang W, Hu N, Lu L (2022) Hybrid poly-ether/carbonate ester electrolyte engineering enables high oxidative stability for quasi-solid-state lithium metal batteries. *Mater Today Nano* 23:100893
19. Wan J, Xie J, Mackanic DG, Burke W, Bao Z, Cui Y (2018) Status, promises, and challenges of nanocomposite solid-state electrolytes for safe and high performance lithium batteries. *Mater Today Nano* 4:1–16
20. Budi A, Basile A, Opletal G, Hollenkamp AF, Best AS, Rees RJ, Bhatt AI, Mullane A, Russo SP (2012) Study of the initial stage of solid electrolyte interphase formation upon chemical reaction of lithium metal and *N*-methyl-*N*-propyl pyrrolidinium-bis(fluorosulfonyl)imide. *J Phy Chem C* 116:19789–19797
21. Zhang S, Xu K, Jow R (2002) Study of LiBF₄ as an electrolyte salt for a Li-ion battery. *J Electrochem Soc* 149:586–590
22. Rey I, Lassegues JC, Grondin J, Servant L (1998) Infrared and Raman study of the PEO-LiTFSI polymer electrolyte. *Electrochim Acta* 43:1505–1510
23. Han H, Zhou S, Zhang D, Feng S, Li L, Liu K, Feng W, Nie J, Hong L, Huang X, Armand M, Zhou Z (2011) Lithium bis(fluorosulfonyl)imide (LiFSI) as conducting salt for nonaqueous liquid electrolytes for lithium-ion batteries: physicochemical and electrochemical properties. *J Power Sources* 196:3623–3632
24. Ue M, Takeda M, Takehara M, Mori S (1997) Electrochemical properties of quaternary ammonium salts for electrochemical capacitors. *J Electrochem Soc* 44:2684–2688
25. Miao RR, Yang J, Feng XJ, Jia H, Wang JL, Nuli Y (2014) Novel dual-salts electrolyte solution for dendrite-free lithium-metal based rechargeable batteries with high cycle reversibility. *J Power Source* 271:291–297
26. Choi SW, Jo SM, Lee WS, Kim YR (2003) An electrospun poly(vinylidene fluoride) nanofibrous membrane and its battery applications. *Adv Mater* 15:2027–2032
27. Ramya CS, Selvasekarapandian S, Hirankumar G, Savitha T, Angelo PC (2008) Investigation on dielectric relaxations of PVP-NH₄SCN polymer electrolyte. *J Non-Cryst Solids* 354:1494–1502
28. Croce F, Focarete ML, Hassoun J, Meschinia I, Scrosati B (2011) A safe, high-rate and high-energy polymer lithium-ion battery based on gelled membranes prepared by electrospinning. *Energy Environ Sci* 4:921–927
29. Zhang H, Liu CY, Zheng LP, Xu F, Feng WF, Li H, Huang XJ, Armand M, Nie J, Zhou ZB (2014) Lithium bis(fluorosulfonyl)imide/poly(ethylene oxide) polymer electrolyte. *Electrochim Acta* 133:529–538
30. Gadjourova Z, Andreev YG, Tunstall DP, Bruce PG (2001) Ionic conductivity in crystalline polymer electrolytes. *Nature* 412:520–523
31. Sun B, Xu C, Mindemark J, Gustafsson T, Edstrom K, Brandell D (2015) At the polymer electrolyte interfaces: the role of the polymer host in interphase layer formation in Li-batteries. *J Mater Chem A* 3:13994–14000
32. Xu C, Sun B, Gustafsson T, Edstrom K, Brandell D, Hahlin M (2014) Interface layer formation in solid polymer electrolyte lithium batteries: an XPS study. *J Mater Chem A* 2:7256–7264
33. Shkrob IA, Martin TW, Zhu Y, Abraham DP (2014) Why bis(fluorosulfonyl)imide is a “magic anion” for electrochemistry. *J Phy Chem C* 118:19661–19671
34. Gu WT, Borodin O, Zdyrko B, Lin HT, Kim H, Nitta N, Huang JX, Magasinski A, Milicev Z, Berdichevsky G, Yushin G (2016) Lithium-iron fluoride battery with in situ surface protection. *Adv Funct Mater* 26:1507–1516
35. Eshetu GG, Diemant T, Grugeon S, Behm RJ, Laruelle S, Armand M, Passerini S (2016) In-depth interfacial chemistry and reactivity focused investigation of lithium-imide- and lithium-imidazole-based electrolytes. *ACS Appl Mater Interfaces* 8:16087–16100
36. Suo LM, Xue WJ, Gobet M, Greenbaum SG, Wang C, Chen YM, Yang WL, Li YX, Li J (2018) Fluorine-donating electrolytes enable highly reversible 5-V-class Li metal batteries. *PNAS* 115:1156–1161
37. Pan J, Cheng YT (2015) General method to predict voltage-dependent ionic conduction in a solid electrolyte coating on electrodes. *Phys Rev B* 91:134116

Publisher's Note Springer Nature remains neutral with regard to jurisdictional claims in published maps and institutional affiliations.